Hindawi
International Journal of Mathematics and Mathematical Sciences
Volume 2021, Article ID 3047712, 9 pages
https://doi.org/10.1155/2021/3047712

Research Article

New Robust PCA for Outliers and Heavy Sparse Noises' Detection via Affine Transformation, the $L_{*,w}$ and $L_{2,1}$ Norms, and Spatial Weight Matrix in High-Dimensional Images: From the Perspective of Signal Processing

Peidong Liang,[1] Habte Tadesse Likassa,[2] Chentao Zhang ,[1,3] and Jielong Guo[4]

[1]*Fujian (Quanzhou)-HIT Research Institute of Engineering and Technology, Quanzhou 362000, China*
[2]*Department of Statistics, College of Natural and Computational Sciences, Addis Ababa University, Addis Ababa, Ethiopia*
[3]*Department of Instrumental and Electrical Engineering, Xiamen University, Xiamen, China*
[4]*Fujian Institute of Research on the Structure of Matter Fuzhou, Chinese Academy of Sciences, Fuzhou, China*

Correspondence should be addressed to Chentao Zhang; 2265275624@qq.com

Received 3 July 2021; Accepted 9 September 2021; Published 28 September 2021

Academic Editor: Niansheng Tang

In this paper, we propose a novel robust algorithm for image recovery via affine transformations, the weighted nuclear, $L_{*,w}$, and the $L_{2,1}$ norms. The new method considers the spatial weight matrix to account the correlated samples in the data, the $L_{2,1}$ norm to tackle the dilemma of extreme values in the high-dimensional images, and the $L_{*,w}$ norm newly added to alleviate the potential effects of outliers and heavy sparse noises, enabling the new approach to be more resilient to outliers and large variations in the high-dimensional images in signal processing. The determination of the parameters is involved, and the affine transformations are cast as a convex optimization problem. To mitigate the computational complexity, alternating iteratively reweighted direction method of multipliers (ADMM) method is utilized to derive a new set of recursive equations to update the optimization variables and the affine transformations iteratively in a round-robin manner. The new algorithm is superior to the state-of-the-art works in terms of accuracy on various public databases.

1. Introduction

Robust methods have been successfully applied to numerous computer vision tasks, including face recognition [1], signal processing, scene categorization [2], point cloud segmentation using image processing [3, 4], and object detection [5]. Image representation, mainly the face recovery and alignment, has been an important research topic and can be found in applications in a variety of areas such as surveillance systems, sparse coding, image denoising, communications, computational imaging, and computer vision [6–12]. However, analyzing visual data is a difficult task due to miscellaneous adverse effects such as illuminations, outliers, and sparse noises. It is thus of importance developing a new approach for image alignment and recovery via a convex optimization, which are resilient to various annoying effects.

Since the inception of the pioneering work of robust principal component analysis (RPCA) by Candes et al. [13], a myriad of algorithms has been addressed for robust sparse-low-rank image recovery, e.g., [14, 15]. However, these methods do not work well when the outliers and heavy sparse noises are heavily skewed. By assuming the dictionary images are registered, Wagneret al. [16] parameterize the misalignment of the test image with an affine transformation. These parameters are optimized using generalized Gauss–Newton methods after linearizing the affine transformation constraints. By minimizing the sparse registration error iteratively and sequentially for each class, their framework is able to deal with a Lagrange of variations in translation, scaling, rotation, and even 3D pose variations. Due to the adoption of holistic features, sparse coding is more robust and less likely to overfit. In [7, 17], a novel algorithm through using sparsity priors for image processing was addressed. To overcome this drawback, Oh et al. [18] considered a new partial singular value thresholding (PSVT) algorithm, which replaced the nuclear norm in RPCA [13] with the partial sum of singular values to improve the recovery of the low-rank part. Lu et al. [19] proposed a tensor robust principal component (T-RPCA) algorithm to find the clean tuber low-rank component. However, T-RPCA is not scalable and robust when the number of tensors becomes large. To tackle the potential effects of outliers and heavy sparse noises and impulse noises, there are several algorithms proposed via different norms, for instance, $L_{2,1}$ norm by weakly convex optimization by [20, 21], L_q norm by [22], and then novel matrix completion technique without a prior rank information by [23–26], which proposed a novel algorithm for image recovery via pruning out the potential impact of outliers and heavy sparse noises. However, the proposed methods need to be improved to become more faithful for image recovery in high-dimensional images particularly in signal processing.

This paper proposes a new robust algorithm via affine transformation, the $L_{*,w}$ and $L_{2,1}$ norms, and spatial weight matrix to reduce the potential impacts of outliers and noises in image and signal processing. To be more resilient to various adverse annoying effects such as occlusions and outliers, the new approach takes the advantages of the novel ideas' affine transformations, $L_{*,w}$ and $L_{2,1}$ norms, for more faithful low-rank sparse image representation. Consequently, the distorted or misaligned images can be rectified by affine transformations to render more accurate robust sparse coding for image representation outcomes. The overall problem is first cast as a convex optimization programming, in which the affine transformations, low-rank sparse coding, and subspace recovery are carried out simultaneously. Additionally, the weighted nuclear norm $L_{*,w}$ and the $L_{2,1}$ norm are also taken into account to prune out the potential impacts of outliers and extreme values from the datasets. Afterward, the iterative reweighted alternating direction method (ADMM) approach is employed and a new set of equations is established to update the optimization variables and affine transformations iteratively in a round-robin manner. Simulation results which were conducted reveal that the proposed approach excels the state-of-the-art works for face recovery on some public datasets. The major contributions of this paper include

(1) The affine transformations involved is used to correct and align distorted or misaligned images so that the proposed method is becoming popular.

(2) The iterative reweighted nuclear norm model along with $L_{2,1}$ norm and the spatial weight matrix is combined to find the true underlying images, as such tackle the potential impacts of outliers and heavy sparse noises in signal processing.

(3) The newly developed method take the potential effects of outliers and heavy sparse noises into account to further propose via the iteratively reweighted ADMM approach to solve the convex optimization problem, and a new set of updating equations is developed to iteratively update the optimization parameters and affine transformations.

(4) In the new proposed method, the $L_{2,1}$ and weighted nuclear norms are incorporated including the spatial weight matrix instead of the L_1 norm to prune out the potential impacts of noises in the signal processing. Integrating the $L_{2,1}$ and weighted nuclear norms into the low-rank representation to enhance the quality of image recoveries will suppress the effect of noisy data. As a result, our proposed model can be used for image recovery and alignment simultaneously.

(5) We conduct experiments on several benchmark datasets, and the experimental results demonstrate the effectiveness of our new method.

This paper is structured as follows. Section 2 describes the formulation of the new problem. Section 3 illustrates the new set of updating equations to solve the formulated convex optimization problem and experimental simulation results are provided in Section 4 to justify the effectiveness of the proposed method. Section 5 draws some concluding remarks to summarize the paper. The summary indicating the comparison of the proposed method with other related approaches is summarised in Table 1.

2. Problem Formulation

Consider n images, $\{\mathbf{I}_i^0\} \in \mathfrak{R}^{w\times h}$, $i = 1, \ldots, n$, where w and h denote the weight and height of the images, respectively. All of these images contain the same objects and are highly correlated with each other. In many scenarios, these images are corrupted by occlusions and outliers. We can stack these images into a matrix: $\mathbf{M} = [\mathrm{vec}(\mathbf{I}_1^0)|\mathrm{vec}(\mathbf{I}_2^0)| \ldots |\mathrm{vec}(\mathbf{I}_n^0)] \in \mathfrak{R}^{m\times n}$, where $\mathrm{vec}(\cdot)$ denotes the vector stacking operator. We can decompose $\mathbf{M}$ into a summation of a low-rank component and a sparse error matrix [41, 42]: $\mathbf{M} = \mathbf{A} + \mathbf{E}$, where $\mathbf{A} \in \mathfrak{R}^{m\times n}$ is a clean low-rank and $\mathbf{E} \in \mathfrak{R}^{m\times n}$ denotes a sparse error matrix incurred by outliers or corruptions.

In practice, $\mathbf{I}_i^0$ are generally not well aligned, entailing the above low-rank sparse decomposition to be imprecise. To take account of this, inspired by [39, 43, 44], we apply affine transformations τ_i to the potentially misaligned input images $\mathbf{I}_i^0$ to get a collection of transformed images $\mathbf{I}_i = \mathbf{I}_i^0 o \tau_i$, where the operator o indicates the transformation. We can then stack these aligned images into a matrix and obtain $\mathbf{M}_{\mathbf{o}\tau} = [\mathrm{vec}(\mathbf{I}_1)|\mathrm{vec}(\mathbf{I}_2)| \ldots |\mathrm{vec}(\mathbf{I}_n)] \in \mathfrak{R}^{m\times n}$. The aligned images can be treated as samples taken from a union of low-dimensional subspaces, which, if well aligned, should exhibit a low-rank subspace structure as the rank of the transformed images is as small as possible, up to some outliers and heavy sparse errors. Solving for the variables corresponding to the constraints $\mathbf{M}_{\mathbf{o}\tau} = \mathbf{A} + \mathbf{E}$ is intractable due to its nonlinearity. To resolve this dilemma, we assume that the change produced by these affine transformations τ_i is small and an initial of τ_i is known. We can then linearize $\mathbf{M}_{o\tau}$ by using the first-order Taylor approximation as $\mathbf{M}_{o(\tau+\Delta\tau)} \approx \mathbf{M}_{\mathbf{o}\tau} + \sum_{i=1}^{n} \mathbf{J}_i \Delta\tau \mathbf{v}_i \mathbf{v}_i^T$, where $\mathbf{M}_{\mathbf{o}\tau} \in \mathfrak{R}^{m\times n}$ is the transformed image, $\Delta\tau \in \mathfrak{R}^{p\times n}$ with p being the number of variables,

Table 1: Comparison of the proposed approach with other related algorithms in terms of the objective function and constraints.

Methods	Objective function	Constraints
[27–30]	$\min_{\mathbf{A},E}\|\mathbf{A}\|_* + \lambda\|\mathbf{E}\|_1$	$\mathbf{M} = \mathbf{A} + \mathbf{E}$
[22, 31–34]	$\min_{\mathbf{A},\mathbf{E}}\|\mathbf{A}\|_* + \lambda\|\mathbf{E}\|_1$	$\mathbf{M}_{\mathbf{o}\tau} + \sum_{i=1}^{n} \mathbf{J}_i\Delta\tau\mathbf{v}_i\mathbf{v}_i^T = \mathbf{A} + \mathbf{E}$
[9, 35, 36]	$\min_{\mathbf{C},\mathbf{E},\mathbf{Q},\mathbf{A}}\|\mathbf{C}\|_* + \lambda\|\mathbf{E}\|_{2,1}$	$\mathbf{M} = \mathbf{AC} + \mathbf{E}, \mathbf{C} = \mathbf{Q}$
[36–40]	$\min_{\mathbf{A},\mathbf{E},\mathbf{C},\mathbf{Q},\Delta\tau}\|\mathbf{A}\|_* + \|\mathbf{C}\|_* + \lambda_1\|\mathbf{Q}\|_{2,1} + \lambda_2\|\mathbf{E}\|_{2,1}$	$\mathbf{M}_{\mathbf{o}\tau} + \sum_{i=1}^{n} \mathbf{J}_i\Delta\tau\mathbf{v}_i\mathbf{v}_i^T = \mathbf{AC} + \mathbf{E}, \mathbf{C} = \mathbf{Q}, \mathbf{Q}\succcurlyeq 0$
Proposed method	$\min_{\mathbf{A},\mathbf{E}}, \Delta\tau w_1\|\mathbf{A}\|_{*,w} + w_2\lambda_1\|\mathbf{E}\|_{2,1}$	$\mathbf{M}_{\mathbf{o}\tau} + \sum_{i=1}^{n} \mathbf{J}_i\Delta\tau\mathbf{v}_i\mathbf{v}_i^T = \mathbf{A} + \mathbf{E}$

$\mathbf{J}_i = (\partial\text{vec}(\mathbf{I}_i\mathbf{o}\tau_i)/\partial\tau_i) \in \mathfrak{R}^{m\times p}$ denotes the Jacobian of the i^{th} image with respect to τ_i, and $\mathbf{v}_i$ is the standard basis for $\mathfrak{R}^n$. In this way, we obtain approximate transformations to recover the low-rank component and sparse noises from high-dimensional images.

To make the new approach more resilient to outliers and heavy sparse noises, the $L_{2,1}$ norms, which combines the advantages of the L_1 and L_2 norms, are used to manifest the sparsity and the low-rank properties. It can also tackle the sparse errors in data points which are highly correlated across all data points in the images. In [8, 38], the joint dictionary learning methods are used but the issue of the affine transformation is not considered, [45, 46], while used an image transformation without considering the $L_{2,1}$ and weighted nuclear norms. Moreover, the $L_{2,1}$ regularizer is considered as the rotational invariant of the L_1 norm and handles the collineraity between features, which is preferred to overcome the difficulty of robustness to outliers [47, 48]. In an effort to overcome inherent shortcoming of the nuclear norm, that is, the equal penalization of each singular value regardless of its magnitude [13], a weighted nuclear norm is based on similar premises to those of the weighted version of the l_1 norm [49] and has been proven to provide significant merits in terms of data recovery performance. Our objective is to recover the low-rank component and sparse components exactly solving a convex program whose objective is combination of the weighted nuclear norm the $L_{1,2}$ norms. By incorporating the weighted nuclear and $L_{2,1}$ norms along with a set of affine transformations and through further considering the spatial weight matrix into account also boosts the performance of algorithm tackling the potential impacts of outliers, noises, and heavy sparse noises between images also, the new method can thus be posted as a convex optimization problem with

$$\min_{\mathbf{A},\mathbf{E},\Delta\tau} w_1\|\mathbf{A}\|_{*,w} + w_2\lambda_1\|\mathbf{E}\|_{2,1}$$
$$\text{s.t}\ \mathbf{M}_{\mathbf{o}\tau} + \sum_{i=1}^{n} \mathbf{J}_i\Delta\tau\mathbf{v}_i\mathbf{v}_i^T = \mathbf{A} + \mathbf{E}, \tag{1}$$

where $\|\mathbf{A}\|_{*,w} = \sum_{i=1}^{\min(m,n)} w_i\sigma_i(\mathbf{A})$ denotes the weighted version of the nuclear norm of $\mathbf{A}$, in which $\sigma_i(\mathbf{A})$ indicates the singular values of $\mathbf{A}$, λ_1 denotes the regularization parameters, and $\|\mathbf{E}\|_{2,1} = \sum_{i=1}^{n}(\sum_{j=1}^{m}\mathbf{E}_{ji}^2)^{1/2}$denotes the $L_{2,1}$ norm of $\mathbf{E}$, and $\mathbf{w}_1$ and $\mathbf{w}_2$ are used to balance the importance of the two types of low-rank priors. Analytically shown in [49], the weighted nuclear norm is convex. An interesting case arises when a reweighted version of this is adopted by defining the weights as follows:

$$\mathbf{w}_\mathbf{i} = \frac{1}{\delta_i(\mathbf{A}) + \boldsymbol{\varepsilon}}, \tag{2}$$

where ε is a small constant. It should be noted that, by setting $\mathbf{w}_\mathbf{i}$, the weighted nuclear norm becomes concave penalizing more heavily smaller values and less the larger ones, and the first weighted nuclear norm term in (1) imposes the low-rank component lying in the low-dimensional subspaces. The fourth term regularizes the error $\mathbf{E}$ to be sparse.

3. Proposed Algorithm

To solve the convex optimization problem in (1), we consider the augmented Lagrangian function given by

$$\mathscr{L}(\mathbf{A},\mathbf{E},\Delta\tau) = \mathbf{w}_1\|\mathbf{A}\|_{*,w} + \mathbf{w}_2\lambda_1\|\mathbf{E}\|_{2,1} + \langle\mathbf{Z}_1, \mathbf{B} - \mathbf{A} - \mathbf{E}\rangle + \frac{\mu_1}{2}\|\mathbf{B} - \mathbf{A} - \mathbf{E}\|_F^2, \tag{3}$$

where $\mathbf{Z}_1 \in \mathfrak{R}^{m\times n}$ is the Lagrangian multipliers, μ_1 and μ_2 are the penalty parameters, and $\mathbf{B} = \mathbf{M}_{\mathbf{o}\tau} + \sum_{i=1}^{n} \mathbf{J}_i\Delta\tau\mathbf{v}_i\mathbf{v}_i^T$. Equation (3) is convex as it depends on the nonnegative matrix factorization. By using augmented Lagrange multiplier with adaptive penalty [50], equation (2) can be rewritten as

$$\mathscr{L}(\mathbf{A},\mathbf{E},\Delta\tau) = w_1\|\mathbf{A}\|_{*,w} + w_2\lambda_1\|\mathbf{E}\|_{2,1} + \frac{\mu_1}{2}\left\|\mathbf{B} - \mathbf{A} - \mathbf{E} + \frac{\mathbf{Z}_1}{\mu_1}\right\|_F^2. \tag{4}$$

Solving (2) directly is computationally prohibitive; thereby, we consider to iteratively update the variables alternatively via alternating iteratively reweighted direction method of multipliers (ADMM) method [51]. In this section, we present a geometric robust subspace algorithm to minimize the recovering errors as defined in equation (1). It is well known that the robust subspace geometric algorithm assisted by the weighted nuclear norm affine transformation, and the $L_{2,1}$ norms boost the performance of the proposed method.

Firstly, to update $\mathbf{A}$, we fix $\mathbf{E}$ and $\Delta\tau$, so $\mathbf{A}^{(k+1)}$ can be determined by

$$\mathbf{A}^{(k+1)} = \arg\min_{\mathbf{A}} \mathscr{L}\left\{\mathbf{A}, \mathbf{E}^{(k)}, \Delta\tau^{(k)}\right\}, \tag{5}$$

where k is the iteration index. By ignoring all irrelevant terms of $\mathbf{A}$, equation (5) can be simplified as

$$\mathbf{A}^{(k+1)} = \underset{\mathbf{A}}{\operatorname{argmin}}\left\{ w_1\|\mathbf{A}\|_{*,w} + \frac{\mu_1^{(k)}}{2}\left\|\mathbf{B}^{(k)} - \mathbf{A} - \mathbf{E}^{(k)} + \frac{\mathbf{Z}_1^{(k)}}{\mu_1^{(k)}}\right\|_F^2 \right\}. \tag{6}$$

We can then use the linear augmented direction method with the soft shrinkage operator in [41] and update $\mathbf{A}^{(k+1)}$ by (6).

Secondly, to update $\mathbf{E}$, we keep $\mathbf{A}$ and $\Delta\tau$ as constants, so $\mathbf{E}^{(k+1)}$ can be determined by

$$\mathbf{E}^{(k+1)} = \underset{\mathbf{E}}{\operatorname{argmin}}\, \mathscr{L}\left\{ \mathbf{A}^{(k+1)}, \mathbf{E}, \Delta\boldsymbol{\tau}^{(k)} \right\}. \tag{7}$$

Again, by ignoring all irrelevant terms of $\mathbf{E}$, equation (7) can be simplified as

$$\mathbf{E}^{(k+1)} = \underset{\mathbf{E}}{\operatorname{argmin}}\left\{ w_2\lambda_1\|\mathbf{E}\|_{2,1} + \frac{\mu_1^{(k)}}{2}\left\|\mathbf{B}^{(k)} - \mathbf{E} + \frac{\mathbf{Z}_1^{(k)}}{\mu_1^{(k)}}\right\|_F^2 \right\}. \tag{8}$$

By using lemma [52], the update of the i^{th} column of $\mathbf{E}^{(k+1)}$ and $\mathbf{E}_i^{(k+1)}$ is given by

$$\mathbf{E}_i^{(k+1)} = \begin{cases} \dfrac{\left\|\mathbf{V}_i^{(k)}\right\|_2 - \left(W_2\lambda_2/\mu_1^{(k)}\right)}{\left\|\mathbf{V}_i^{(k)}\right\|_2}\mathbf{V}_i^{(k)}, & \text{if } \left\|\mathbf{V}_i^{(k)}\right\|_2 \geq \dfrac{w_2\lambda_1}{\mu_1^{(k)}}, \\ 0, & \text{otherwise}, \end{cases} \tag{9}$$

where $\|.\|_2$ denotes the Euclidean norm and $\mathbf{V}^{(k)} = (\mathbf{B}^{(k)} - \mathbf{A}^{(k)} + (\mathbf{Z}_1^{(k)}/\mu_1^{(k)}))$.

Lastly, to get an update of $\Delta\tau$, we keep $\mathbf{A}$ and $\mathbf{E}$ as constants, and $\Delta\tau^{(k+1)}$ can be determined by

$$\Delta\boldsymbol{\tau}^{(k+1)} = \underset{\Delta\boldsymbol{\tau}}{\operatorname{argmin}}\, \mathscr{L}\left\{\mathbf{A}^{(k+1)}, \mathbf{E}^{(k+1)}, \Delta\boldsymbol{\tau}\right\}. \tag{10}$$

By ignoring all irrelevant terms of $\Delta\tau$, we can obtain

$$\Delta\boldsymbol{\tau}^{(\mathbf{k}+1)} = \underset{\Delta\boldsymbol{\tau}}{\operatorname{argmin}}\left\{ \frac{\mu_1^{(k)}}{2}\left\|\mathbf{B}^{(k)} - \mathbf{A}^{(k+1)} - \mathbf{E}^{(k+1)} + \frac{\mathbf{Z}_1^{(k)}}{\mu_1^{(k)}}\right\|_F^2 \right\}. \tag{11}$$

Solving (11) with the threshold operators [22, 43], we can get an update of $\Delta\tau^{(k+1)}$ as

$$\Delta\boldsymbol{\tau}^{(k+1)} = \sum_{i=1}^{n} \mathbf{J}_i^{+}\left(\mathbf{A}^{(k+1)} + \mathbf{E}^{(k+1)} - \mathbf{M}_{\mathbf{o}\boldsymbol{\tau}} - \frac{\mathbf{Z}_1^{(k)}}{\mu_1^{(k)}} \right)\mathbf{v}_i\mathbf{v}_i^{T}, \tag{12}$$

where $\mathbf{J}_i^{+}$ denotes the Moore–Penrose pseudoinverse of $\mathbf{J}_i$ [53].

Following the same steps as the above, the Lagrangian multiplier $\mathbf{Z}_1$ is updated by

$$\mathbf{Z}_1^{(k+1)} = \mathbf{Z}_1^{(k)} + \mu_1^{(k+1)}\left\{ \mathbf{B}^{(k)} - \mathbf{A}^{(k+1)} - \mathbf{E}^{(k+1)} \right\}. \tag{13}$$

Likewise, the regularization parameters μ_1 is updated, respectively, by

$$\mu_1^{(k+1)} = \min\left\{\mu_{\max}, \rho\mu_1^{(k)}\right\}, \tag{14}$$

where ρ is a properly chosen constant and $\mu_{\max}$ is a tunable parameter adjusting the convergence of the proposed method. These updating equations proceed in a round-robin manner until convergence.

4. Experimental Simulations

In this section, we evaluate the effectiveness of proposed algorithm on handwritten digits' datasets including the MNIST [54], Dummy Face Images [55], and Algore Video Face images [43]. In this work, novel ideas affine transformation, the spatial weight matrix, the weighted nuclear norm, and the $L_{2,1}$ norms are taken into consideration to boost the performance of the proposed method. Similar to [39, 43], parameters in our experiments are chosen heuristically. Different datasets are taken into account to examine the effectiveness of the proposed method as compared to the baselines' RASL [43] and NQLSD [22]. To further see the performance, the numerical simulations, using the peak signal-noise ratio, are considered. As shown in Table 2, the PSNR is very high for all datasets. To further check the image similarity quantitatively to describe the performance of our algorithm using the statistical measures of similarity, mainly the peak signal-to-noise ratio (PSNR) [56],

$$\text{PSNR}(f, \hat{f}) = 10\log_{10}^{\left(255^2/(1/m\times n)\sum_{i=1}^{m}\sum_{i=1}^{n}\left(f_{ij}-\hat{f}_{ij}\right)^2\right)}, \tag{15}$$

where both the original image f and the recovered image $\hat{f}$ are of size $m \times n$.

4.1. Handwritten Images. In this experiment, different datasets are considered to examine the effectiveness of the proposed method. First, 30 handwritten digits of the size 29×29 are taken from the MNIST database [54]. We compare the PSNR performance of the proposed method with the aforementioned five baselines, as shown in Table 2, from which we can see that NQLSD has better performance than RASL, as NQLSD employs the local linear approximation with a quadratic penalty approach to tackle the potential setback of outliers and sparse noises in the images. The proposed method is superior to the other two baselines, as it considers an iterative linearization via affine transformation, weighted nuclear norm, and spatial weight matrix and considers the $L_{2,1}$ norms. As an illustration, some visual images of the recovered handwritten digits based on the aforementioned methods are shown in Figure 1(d), from which we can see that the proposed method recovers the handwritten images better as compared to the two baselines. We can also observe from Table 2 that the proposed approach provides the best performance.

Table 2: Performance comparisons on various datasets via the peak signal-noise ratio (PSNR) (dB).

Datasets	Proposed method	NQLSD [22]	RASL [43]
Handwritten images	77.41	70.23	69.20
Dummy face images	93.75	89.01	80.45
Al Gore face images	99.51	92.45	90.40
Natural face images	105.89	102.003	89.66
Complicated images	123.47	120.03	118.05

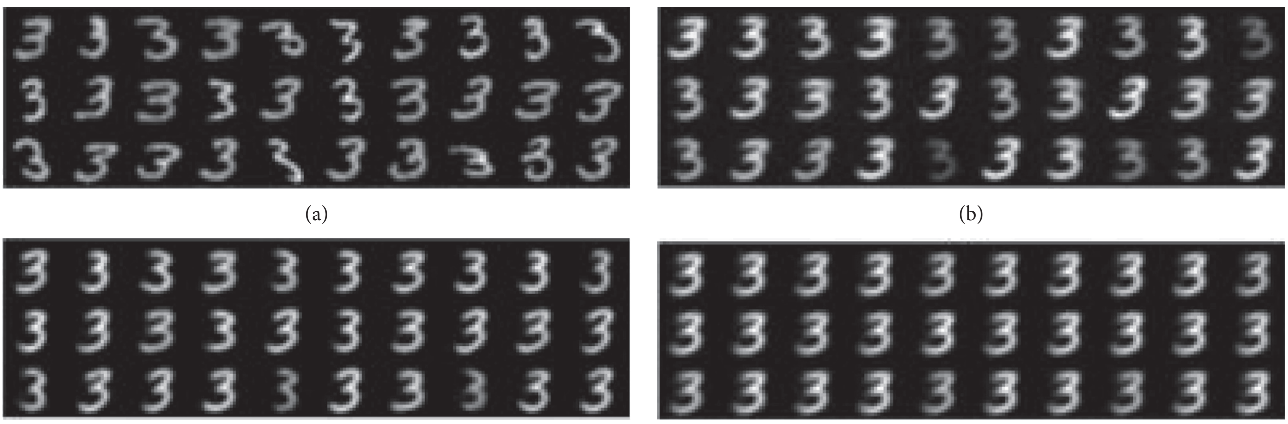

(a) (b) (c) (d)

Figure 1: Some recovered handwritten digits. (a) Original, (b) NQLSD, (c) RASL, and (d) proposed method.

4.2. Dummy Face Images. To further check the effectiveness of the proposed method, we consider dummy face images, from which the proposed method is more clear than the other state of the art of the works (see Figure 2(d)). The proposed method is more clear than the other state of the art of the works. To further justify the effectiveness of the proposed method, we computed the PSNRs of the dummy face images where we observe that the proposed method is more boosted than the other two baselines (Table 2). This result is resembled with the results illustrated via visualization.

4.3. Al Gore Video Face Images. Finally, we conduct an experiment on a more complicated face images from videos sequences taken from the Al Gore talking [43]. From these datasets and video sequences, 7 different video face images with the size 232×312 are taken into account, where the simulation results are illustrated in Figure 3(d), from which the performance of the proposed method is visually clearer than the two baselines. The comparison of PSNR using the proposed method along with two baselines is given in Table 2, from which we can see that the NQLSD yields better performance than the RASL. This is because NQLSD combines the penalized and further decomposes the errors than the RASL. We can further note from Table 2 that the proposed method still outperforms all baselines, as it further considers the $L_{2,1}$ norms, weighted spatial matrix, and the affine transformations. This is because affine transformation corrects the distorted images, while the $L_{2,1}$ norms prune out the potential impacts of extreme values and the dilemma of spatial dependency between images tackled via the spatial weight matrix.

4.4. Natural Face Images. Next, we conduct simulations on more challenging images taken from the Labeled Natural Faces database. In this experiment, 7 natural face images with the size 80×60 are considered. We compare the proposed method with the aforementioned two baselines in terms of PSNR for image recovery. The comparison results are given in Table 2, from which we can see that the NQLSD outperforms RASL, as NQLSD considers the penalized parameters than RASL. Again, an illustration, some recovered natural face images based on the proposed method and aforementioned baselines are given in Figure 4, where the recovered natural face images are depicted in Figure 4(d). The recovered images by the aforementioned algorithms are shown in Figure 4(d), from which we can see that the visual quality of the proposed method is better than all of the baselines. This is in line with the numerical results in Table 2. The performance of the new model is boosted because we incorporated more novel ideas such as the affine transformations, the weighted nuclear norm, and the $L_{2,1}$ norm incorporating the issue of the spatial weight matrix to cast the extreme values.

4.5. Complicated Windows. To further examine the effectiveness of the proposed algorithm, we considered complicated windows, as shown in Figure 5(d), from which we can recognize that the proposed method is more clear than the other state of the art of the works. To justify the

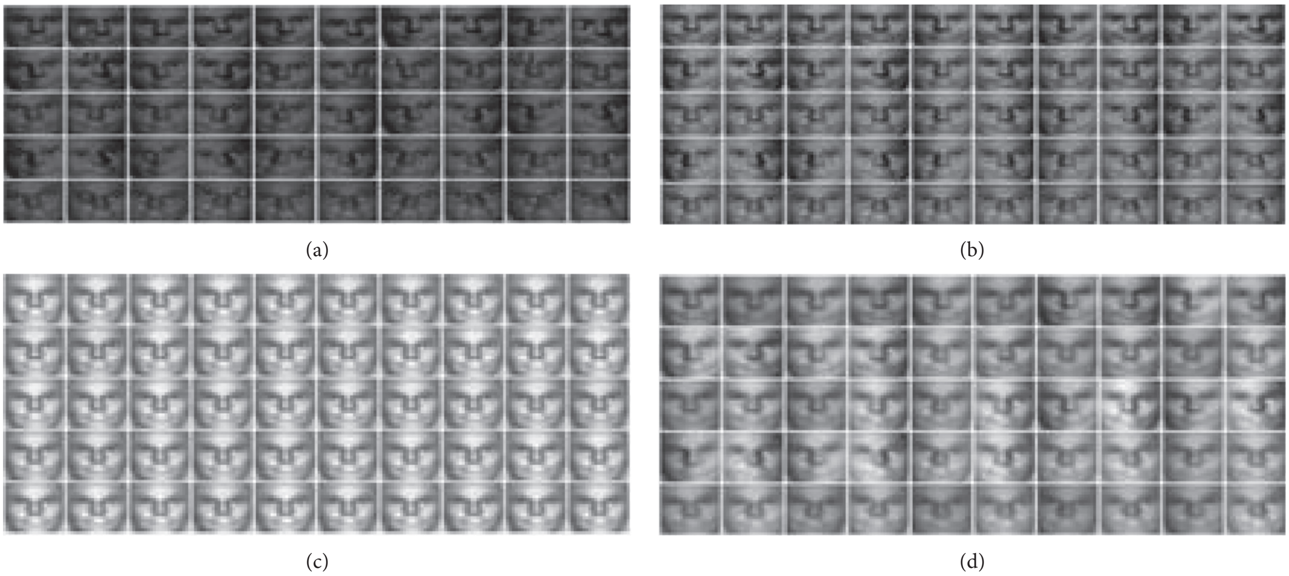

Figure 2: Some recovered dummy face images. (a) Original, (b) NQLSD, (c) RASL, and (d) proposed method.

Figure 3: Some recovered video sequence face images. (a) Original, (b) NQLSD, (c) RASL, and (d) proposed method.

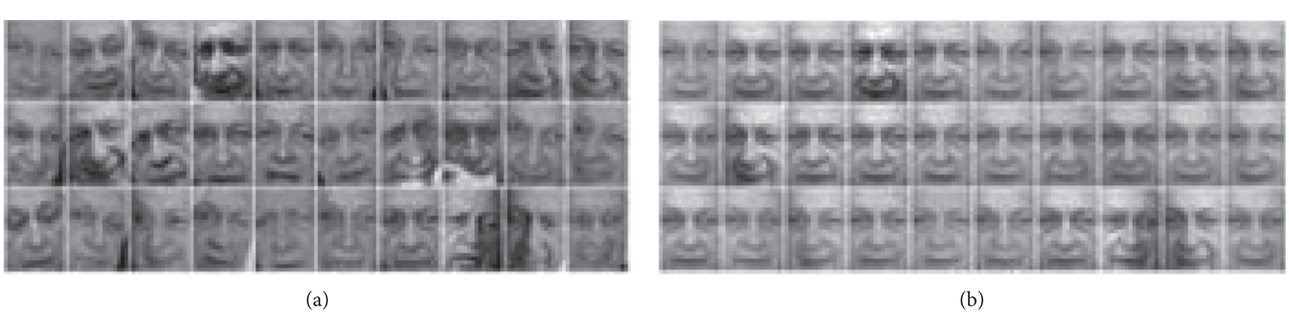

Figure 4: Continued.

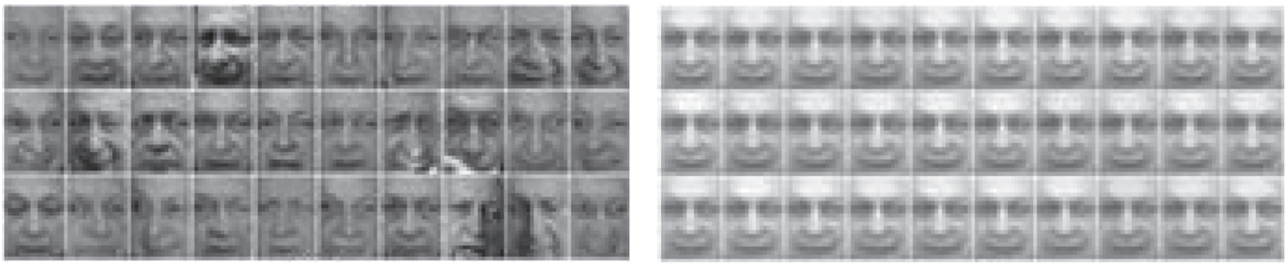

(c) (d)

Figure 4: Some recovered natural face images. (a) Original, (b) NQLSD, (c) RASL, and (d) proposed method.

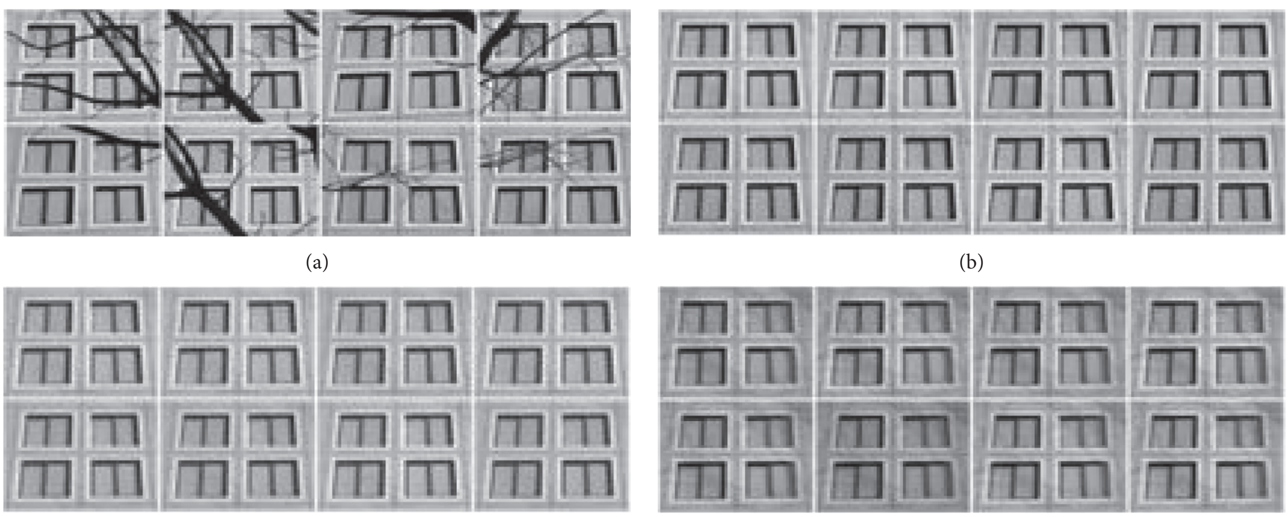

(a) (b) (c) (d)

Figure 5: Some recovered complicated window images. (a) Original, (b) NQLSD, (c) RASL, and (d) proposed method.

effectiveness of the proposed method, numerical experimental simulations justify the performance improvement, as given in Table 2, which justifies that the proposed method is more better than the state of the art of the works. This is because the new method is more resilient with outliers and heavy sparse noises as it is assisted with novel ideas such as the affine transformations, the weighted nuclear norm, and the $L_{2,1}$ norm incorporating the issue of the spatial weight matrix to cast the extreme values.

5. Conclusion

In this paper, a new algorithm is proposed to prune out the potential impacts of gross errors from the corrupted images via affine transformations, the weighted nuclear norm $L_{*,w}$, the $L_{2,1}$ norms, and the spatial weight matrix. Considering all mentioned novel ideas are useful to get a trustful method in the areas of high-dimensional images particularly in signal processing, the optimal parameters corresponding to affine transformations and other potential optimizing parameters involved in a new proposed convex optimization problem are found. The ADMM approach is then employed and a new set of equations is established to alternatively update the optimization variables and the affine transformations. Conducted simulations show that the new method outperforms the state-of-the-art methods in terms of accuracy on five public databases.

Data Availability

The data used to support the findings of the study are available from the corresponding author upon request.

Conflicts of Interest

The authors declare that they have no conflicts of interest.

Acknowledgments

This work was supported by National Key Research and Development Program of China under Grant no. 2018YFB1305700 and Scientific and Technological Program of Quanzhou City under Grant no. 2019CT009. The authors also acknowledge Addis Ababa University, Ethiopia, and the National Science Fund of Young Scholars (Grant no. 61806186), State Key Laboratory of Robotics and System (HIT) (Grant no. SKLRS-2019-kf-15), and the program

"Fujian Intelligent Logistics Industry Technology Research Institute (Grant no. 2018H2001) for their contribution in providing materials that also helped in the research article.

References

[1] J. Wright, A. Y. Yang, A. Ganesh, S. S. Sastry, and Y. Ma, "Robust face recognition via sparse representation," *IEEE Transactions on Pattern Analysis and Machine Intelligence*, vol. 31, no. 2, pp. 210–227, 2008.

[2] J. Yang, K. Yu, Y. Gong, and T. Huang, "Linear spatial pyramid matching using sparse coding for image classification,," in *2009 IEEE Conference on Computer Vision and Pattern Recognition*, pp. 1794–1801, IEEE, Miami, FL, USA, June 2009.

[3] V. Barrile, G. Candela, and A. Fotia, "Point cloud segmentation using image processing techniques for structural analysis," *The International Archives of the Photogrammetry, Remote Sensing and Spatial Information Sciences*, vol. XLII-2, no. W11, pp. 187–193, 2019.

[4] Y. Yan and L. Huang, "Large-scale image processing research cloud," in *Proceedings of the International Conference on Cloud Computing*, pp. 88–93, Prairie View, TX, 2014.

[5] S. Agarwal and D. Roth, "Learning a sparse representation for object detection," in *Proceedings of the European Conference on Computer Vision*, pp. 113–127, Springer, Springer Nature, Switzerland, 2002.

[6] X. Xiang and T. D. Tran, "Linear disentangled representation learning for facial actions," *IEEE Transactions on Circuits and Systems for Video Technology*, vol. 28, no. 12, pp. 3539–3544, 2018.

[7] R. Zhang, F. Nie, X. Li, and X. Wei, "Feature selection with multi-view data: a survey," *Information Fusion*, vol. 50, pp. 158–167, 2019.

[8] X. Wei, H. Shen, Y. Li et al., "Reconstructible nonlinear dimensionality reduction via joint dictionary learning," *IEEE transactions on neural networks and learning systems*, vol. 30, no. 1, pp. 175–189, 2018.

[9] G. Lerman and T. Maunu, "An overview of robust subspace recovery," *Proceedings of the IEEE*, vol. 106, no. 8, pp. 1380–1410, 2018.

[10] D. Huang, M. Storer, F. De la Torre, and H. Bischof, "Supervised local subspace learning for continuous head pose estimation," in *CVPR 2011*, pp. 2921–2928, IEEE, Colorado Springs, CO, USA, June 2011.

[11] V. Drouard, S. Ba, G. Evangelidis, A. Deleforge, and R. Horaud, "Head pose estimation via probabilistic high-dimensional regression,," in *Proceedings of the 2015 IEEE International Conference on Image Processing (ICIP)*, pp. 4624–4628, IEEE, Quebec City, QC, Canada, September 2015.

[12] F. Wen, L. Pei, Y. Yang, W. Yu, and P. Liu, "Efficient and robust recovery of sparse signal and image using generalized nonconvex regularization," *IEEE Transactions on Computational Imaging*, vol. 3, no. 4, pp. 566–579, 2017.

[13] E. J. Candès, X. Li, Y. Ma, and J. Wright, "Robust principal component analysis?" *Journal of the ACM*, vol. 58, no. 3, p. 11, 2011.

[14] S. Ebadi and E. Izquierdo, "Approximated RPCA for fast and efficient recovery of corrupted and linearly correlated images and video frames," in *Proceedings of the International Conference on Systems, Signals and Image Processing (IWSSIP)*, pp. 49–52, IEEE, London, UK, September 2015.

[15] J. Wright, A. Ganesh, S. Rao, Y. Peng, and Y. Ma, "Robust principal component analysis: exact recovery of corrupted low-rank matrices via convex optimization," *Advances in Neural Information Processing Systems*, vol. 58, pp. 2080–2088, 2009.

[16] A. Wagner, J. Wright, A. Ganesh, Z. Zhou, H. Mobahi, and Y. Ma, "Toward a practical face recognition system: robust alignment and illumination by sparse representation," *IEEE Transactions on Pattern Analysis and Machine Intelligence*, vol. 34, no. 2, pp. 372–386, 2011.

[17] X. Wei, H. Shen, and M. Kleinsteuber, "Trace quotient with sparsity priors for learning low dimensional image representations," *IEEE Transactions on Pattern Analysis and Machine Intelligence*, vol. 42, no. 12, pp. 3119–3135, 2019.

[18] T.-H. Oh, Y.-W. Tai, J.-C. Bazin, H. Kim, and I. S. Kweon, "Partial sum minimization of singular values in robust PCA: algorithm and applications," *IEEE Transactions on Pattern Analysis and Machine Intelligence*, vol. 38, no. 4, pp. 744–758, 2016.

[19] C. Lu, J. Feng, Y. Chen, W. Liu, Z. Lin, and S. Yan, "Tensor robust principal component analysis with a new tensor nuclear norm," *IEEE Transactions on Pattern Analysis and Machine Intelligence*, vol. 42, no. 4, pp. 925–938, 2018.

[20] Q. Liu, Y. Gu, and H. C. So, "Doa estimation in impulsive noise via low-rank matrix approximation and weakly convex optimization," *IEEE Transactions on Aerospace and Electronic Systems*, vol. 55, no. 6, pp. 3603–3616, 2019.

[21] Q. Liu, C. Yang, Y. Gu, and H. C. So, "Robust sparse recovery via weakly convex optimization in impulsive noise," *Signal Processing*, vol. 152, pp. 84–89, 2018.

[22] X. Chen, Z. Han, Y. Wang, Y. Tang, and H. Yu, "Nonconvex plus quadratic penalized low-rank and sparse decomposition for noisy image alignment," *Science China Information Sciences*, vol. 59, no. 5, pp. 1–13, 2016.

[23] Q. Liu, X. Li, and J. Yang, "Optimum co-design for image denoising between type-2 fuzzy identifier and matrix completion denoiser," *IEEE Transactions on Fuzzy Systems*, 2020.

[24] B. Shen, R. R. Kamath, and Z. J. K. Hahn Choo, "Robust tensor decomposition based background/foreground separation in noisy videos and its applications in additive manufacturing," *TechRXiv*, 2021.

[25] H. Cai, K. Hamm, L. Huang, and D. Needell, "Robust cur decomposition: theory and imaging applications," 2021, https://arxiv.org/2101.05231.

[26] B. E. Moore, C. Gao, and R. R. Nadakuditi, "Panoramic robust PCA for foreground-background separation on noisy, free-motion camera video," *IEEE Transactions on Computational Imaging*, vol. 5, no. 2, pp. 195–211, 2019.

[27] F. De la Torre and M. J. Black, "Robust parameterized component analysis: theory and applications to 2D facial appearance models," *Computer Vision and Image Understanding*, vol. 91, no. 1-2, pp. 53–71, 2003.

[28] D. T. Nguyen, *Long-rank Approximation and Sparse Recovery for Visual Data Reconstruction*, The Johns Hopkins University, Baltimore, Maryland, 2012.

[29] M. Tao and X. Yuan, "Recovering low-rank and sparse components of matrices from incomplete and noisy observations," *SIAM Journal on Optimization*, vol. 21, no. 1, pp. 57–81, 2011.

[30] R. Vidal, Y. Ma, and S. S. Sastry, *Generalized Principal Component Analysis*, Springer, Berlin, Germany, vol. 5, 2016.

[31] R. Vidal, Y. Ma, and S. S. Sastry, "Robust principal component analysis," *Interdisciplinary Applied Mathematics*, , pp. 63–122, Springer, 2016.

[32] A. Baghaie, R. M. D'souza, and Z. Yu, "Sparse and low rank decomposition based batch image alignment for speckle reduction of retinal OCT images,," in *Proceedings of the 2015 IEEE 12th International Symposium on Biomedical Imaging (ISBI)*, pp. 226–230, IEEE, Brooklyn, NY, USA, April 2015.

[33] H. T. Likassa, W.-H. Fang, and Y.-A. Chuang, "Modified robust image alignment by sparse and low rank decomposition for highly linearly correlated data," in *Proceedings of the 2018 3rd International Conference on Intelligent Green Building and Smart Grid (IGBSG)*, pp. 1–4, IEEE, Yilan, Taiwan, April 2018.

[34] Q. Zheng, Y. Wang, and P.-A. Heng, "Online robust image alignment via subspace learning from gradient orientations," in *Proceedings of the IEEE International Conference on Computer Vision (ICCV)*, pp. 1753–1762, Venice, Italy, October 2017.

[35] S. Xiao, M. Tan, D. Xu, and Z. Y. Dong, "Robust kernel low-rank representation," *IEEE transactions on neural networks and learning systems*, vol. 27, no. 11, pp. 2268–2281, 2015.

[36] G. Liu, Z. Lin, S. Yan, J. Sun, Y. Yu, and Y. Ma, "Robust recovery of subspace structures by low-rank representation," *IEEE Transactions on Pattern Analysis and Machine Intelligence*, vol. 35, no. 1, pp. 171–184, 2012.

[37] G. R. Obozinski, M. J. Wainwright, and M. I. Jordan, "High-dimensional support union recovery in multivariate regression," *Advances in Neural Information Processing Systems*, vol. 21, pp. 1217–1224, 2009.

[38] X. Wei, Y. Li, H. Shen, F. Chen, M. Kleinsteuber, and Z. Wang, "Dynamical textures modeling via joint video dictionary learning," *IEEE Transactions on Image Processing*, vol. 26, no. 6, pp. 2929–2943, 2017.

[39] H. T. Likassa, "New robust principal component analysis for joint image alignment and recovery via affine transformations, frobenius and norms," *International Journal of Mathematics and Mathematical Sciences*, vol. 2020, Article ID 8136384, 9 pages, 2020.

[40] H. T. Likassa, W.-H. Fang, and J.-S. Leu, "Robust image recovery via affine transformation and $L_{2,1}$ norm," *IEEE Access*, vol. 7, pp. 125011–125021, 2019.

[41] Z. Lin, M. Chen, and Y. Ma, "TThe augmented lagrange multiplier method for exact recovery of corrupted low-rank matrices," 2010, https://arxiv.org/1009.5055.

[42] G. Liu, Z. Lin, and Y. Yu, "Robust subspace segmentation by low-rank representation," in *Proceedings of the 27th International Conference on Machine Learning (ICML-10)*, Haifa, Israel, 2010.

[43] Y. Yigang Peng, A. Ganesh, J. Wright, W. Wenli Xu, and Y. Yi Ma, "RASL: robust alignment by sparse and low-rank decomposition for linearly correlated images," *IEEE Transactions on Pattern Analysis and Machine Intelligence*, vol. 34, no. 11, pp. 2233–2246, 2012.

[44] H. T. Likassa, W. Xian, and X. Tang, "New robust regularized shrinkage regression for high-dimensional image recovery and alignment via affine transformation and tikhonov regularization," *International Journal of Mathematics and Mathematical Sciences*, vol. 2020, Article ID 1286909, 10 pages, 2020.

[45] X. Wei, Y. Li, H. Shen, W. Xiang, and Y. Lu Murphey, "Joint learning sparsifying linear transformation for low-resolution image synthesis and recognition," *Pattern Recognition*, vol. 66, pp. 412–424, 2017.

[46] H. T. Likassa and W.-H. Fang, "Robust regression for image alignment via subspace recovery techniques," in *Proceedings of the 2018 VII International Conference on Network, Communication and Computing*, pp. 288–293, 2018.

[47] T. Bouwmans, A. Sobral, S. Javed, S. K. Jung, and E.-H. Zahzah, "Decomposition into low-rank plus additive matrices for background/foreground separation: a review for a comparative evaluation with a large-scale dataset," *Computer Science Review*, vol. 23, pp. 1–71, 2017.

[48] C. Ding, D. Zhou, X. He, and H. Zha, "R_1-PCA: rotational invariant L_1-norm principal component analysis for robust subspace factorization," in *Proceedings of the 23rd International Conference on Machine Learning (ICML)*, pp. 281–288, Berkeley, CA, 2006.

[49] S. Gu, L. Zhang, W. Zuo, and X. Feng, "Weighted nuclear norm minimization with application to image denoising," in *Proceedings of the IEEE Conference on Computer Vision and Pattern Recognition*, pp. 2862–2869, Columbus, OH, USA, June 2014.

[50] R. Subbarao and P. Meer, "Beyond RANSAC: user independent robust regression," in *2006 Conference on Computer Vision and Pattern Recognition Workshop (CVPRW'06)*, p. 101, June 2006.

[51] S. Boyd, N. Parikh, E. Chu, B. Peleato, and J. Eckstein, "Distributed optimization and statistical learning via the alternating direction method of multipliers," *Foundations and Trends® in Machine Learning*, vol. 3, no. 1, pp. 1–122, 2011.

[52] J. Yang and Y. Zhang, "Alternating algorithms for 1-problems in compressive sensing," Tech. Rep. TR09-37, Rice University CAAM, Houston, TX, 2010.

[53] P. Courrieu, "Fast computation of moore-penrose inverse matrices," 2008, https://arxiv.org/0804.4809.

[54] Y. LeCun, L. Bottou, Y. Bengio, and P. Haffner, "Gradient-based learning applied to document recognition," *Proceedings of the IEEE*, vol. 86, no. 11, pp. 2278–2324, 1998.

[55] G. B. Huang, M. Ramesh, T. Berg, and E. Learned-Miller, *Labeled Faces in the Wild: A Database for Studying Face Recognition in Unconstrained Environments*, University of Massachusetts, Amherst, MA, USA, 2007.

[56] A. Hore and D. Ziou, "Image quality metrics: PSNR vs SSIM," in *2010 20th International Conference on Pattern Recognition*, pp. 2366–2369, IEEE, Istanbul, Turkey, August 2010.